SLEEPJ, 2020, 1–12

doi: 10.1093/sleep/zsz210
Advance Access Publication Date: 8 November 2019
Original Article

ORIGINAL ARTICLE

Wakefulness/sleep architecture and electroencephalographic activity in mice lacking the translational repressor 4E-BP1 or 4E-BP2

Cassandra C. Areal[1,2], Ruifeng Cao[3,4], Nahum Sonenberg[5] and Valérie Mongrain[1,2,*]

[1]Research Center and Center for Advanced Research in Sleep Medicine, Hôpital du Sacré-Coeur de Montréal (CIUSSS-NIM), Montreal, Québec, Canada, [2]Department of Neuroscience, Université de Montréal, Montreal, Québec, Canada, [3]Department of Biomedical Sciences, University of Minnesota Medical School, Duluth, MN, [4]Department of Neuroscience, University of Minnesota Medical School, Minneapolis, MN and [5]Department of Biochemistry and Goodman Cancer Research Center, McGill University, Montreal, Québec, Canada

*Corresponding author. Valérie Mongrain, Research Center and Center for Advanced Research in Sleep Medicine, Hôpital du Sacré-Coeur de Montréal (CIUSSS-NIM), 5400 Gouin West blvd., Montreal, Québec H4J 1C5, Canada. Email: valerie.mongrain@umontreal.ca

Abstract

Sleep and sleep loss are affecting protein synthesis in the brain, but the contribution of translational control to wakefulness and sleep regulation remains poorly understood. Here, we studied the role of two suppressors of protein synthesis, the eukaryotic translation initiation factor 4E-binding proteins 1 and 2 (4E-BP1 and 4E-BP2), in sleep architecture and electroencephalographic (EEG) activity as well as in the EEG and molecular responses to acute sleep loss. The EEG of mice mutant for the genes encoding 4E-BP1 or 4E-BP2 (*Eif4ebp1* and *Eif4ebp2* knockout [KO] mice) was recorded under undisturbed conditions and following a 6-hour sleep deprivation (SD). The effect of SD on the expression of genes known to respond to SD was also measured in the prefrontal cortex of *Eif4ebp1* and *Eif4ebp2* KO mice. *Eif4ebp1* KO mice differed from wild-type mice in parameters of wakefulness and sleep quantity and quality, and more subtly in the gene expression response to SD. For instance, *Eif4ebp1* KO mice spent more time in slow-wave sleep (SWS) and showed altered baseline 24-h time courses of SWS delta (1–4 Hz) activity and sigma (10–13 Hz) activity. *Eif4ebp2* KO mice differed from wild-type mice only for wakefulness and sleep quality, expressing changes in EEG spectral activity generally revealed during and after SD. These findings suggest different roles of effectors of translational control in the regulation of wakefulness and sleep and of synchronized cortical activity.

Statement of Significance

Protein synthesis is affected by wakefulness/sleep history, but a role for translational control in the regulation of wakefulness/sleep remains to be established. We found that the absence of one translational repressor, 4E-BP1, affects wakefulness/sleep architecture and the normal dynamics of electroencephalographic activity during wakefulness and sleep, and that the absence of a second translational repressor, 4E-BP2, generally increases wakefulness/sleep electroencephalographic activity under sleep-deprived conditions while leaving architecture unaffected. These results suggest different roles of two related regulators of protein synthesis in the control of wakefulness/sleep amount and quality. Given the importance of translational control in brain physiology and diseases such as autism, epilepsy, and tuberous sclerosis complex, our findings point to pathways contributing to sleep disturbances in neuropathology.

Key words: protein synthesis; electroencephalography; spectral analysis; sleep deprivation; gene expression

Submitted: 8 February, 2019; **Revised:** 5 August, 2019

Introduction

Sleep is highly conserved across species and is essential for proper brain functioning. Alterations in the sleep–wake cycle are known to be a symptom of many neurological and psychiatric diseases, such as autism spectrum disorders [1, 2]. It is generally recognized that two main processes are controlling sleep: (1) a homeostatic process that determines sleep intensity in relation to the duration of prior wakefulness and (2) a circadian process defining rhythmic periods of low- and high-sleep propensity across the 24 hours [3, 4]. Specific features of sleep have been shown to be predominantly influenced in a homeostatic or a circadian manner and have been used, respectively, as markers of the homeostatic or the circadian process. For instance, changes in sleep intensity quantified using delta (1–4 Hz) activity during slow-wave sleep (SWS) reflects homeostatic sleep pressure, whereas the proportion of total sleep occupied by paradoxical sleep (PS) and theta (4–7 Hz) activity during PS mostly depend on circadian time [5, 6].

Sleep and sleep loss regulate gene transcription and protein synthesis and shape plastic structural changes in the central nervous system [7, 8]. Sleep is indeed known to elevate messenger RNA (mRNA) levels of genes associated with protein synthesis in the cerebral cortex and hippocampus [9, 10], and SWS in particular was shown to correlate with increased protein synthesis [11, 12]. In an opposite manner, sleep deprivation (SD) negatively affects genes important for translation [13]. Moreover, SD attenuates mechanistic target of rapamycin (mTOR) complex 1-dependent protein synthesis [14], and inhibition of mTOR-dependent protein synthesis was shown to abolish sleep-dependent plasticity in the cerebral cortex [15]. However, even if there is considerable support for a modulatory role of sleep on mechanisms controlling translation, little is known concerning the potential role of the protein synthesis machinery in the regulation of wakefulness and sleep.

Protein synthesis is predominantly regulated at the stage of translation initiation, as a critical step in the initiation of translation is the recognition of the mRNA 5′ cap by the eukaryotic translation initiation factor 4E (eIF4E) [16]. Translation initiation is repressed by eIF4E-binding proteins (4E-BPs), which prevent binding of eIF4E to the eIF4G subunit of the translation initiation complex [16, 17]. The phosphorylation of 4E-BPs by mTOR results in the dissociation of 4E-BPs from eIF4E and thus promotes 5′ cap-dependent protein synthesis [16–18]. During nervous system development, mTOR fulfills numerous roles, notably in neuronal survival and differentiation, neurite growth, and synaptogenesis [19]. In the adult brain, mTOR regulates many forms of neuronal plasticity [15, 16, 19], thus playing roles in learning and memory. Nevertheless, the role of mTOR and 4E-BPs in the regulation of wakefulness and sleep amount and quality remains unclear.

In mammals, three 4E-BPs have been identified (i.e. 4E-BP1, 4E-BP2, and 4E-BP3) [17], with murine 4E-BP1 and 4E-BP2 sharing 60% identity [20]. The gene coding for 4E-BP1 (i.e. *Eif4ebp1*) is expressed in most tissues with the highest expression in skeletal muscle and pancreas, and low expression in the brain [20]. Strikingly, 4E-BP1 is found in the suprachiasmatic nucleus (SCN) of the hypothalamus, where its phosphorylation varies with internal (circadian) time, and mice lacking 4E-BP1 (knockout [KO]) show functional alterations in the central circadian clock [21]. The gene coding for 4E-BP2 (i.e. *Eif4ebp2*) is more abundantly expressed in the brain [20], where it was shown to regulate hippocampal synaptic plasticity and hippocampus-dependent memory [22]. In addition, *Eif4ebp2* KO mice display an increased ratio of excitatory to inhibitory synaptic transmission, which is associated with autistic-like behaviors such as deficits in social interaction and repetitive behaviors [23]. This indicates that *Eif4ebp2* KO mice could exhibit a sleep phenotype similar to patients with autism spectrum disorders, which is characterized by decreased sleep consolidation and SWS [1, 2].

We have investigated here the role of the translational repressors 4E-BP1 and 4E-BP2 in wakefulness and sleep regulation and their implication in the molecular response to sleep loss. We measured vigilance state duration and quality with electroencephalographic/electromyographic (EEG/EMG) recordings and EEG spectral activity in *Eif4ebp1* and *Eif4ebp2* KO mice, with a particular focus on EEG markers of the homeostatic and circadian processes of sleep regulation. The response to a homeostatic challenge was thus measured using recordings performed during and after SD. Last, the homeostatic response to SD was further evaluated by measuring gene expression in the cerebral cortex of *Eif4ebp1* and *Eif4ebp2* KO mice by interrogating specific genes targeted for their recognized response to SD [9, 10, 13], using quantitative polymerase chain reaction (qPCR). The findings demonstrate that 4E-BP1 plays a role in the regulation of wakefulness and sleep quantity and quality and that 4E-BP2 plays a role in the regulation of wakefulness and sleep EEG quality.

Methods

Animals and protocol

Eif4ebp1$^{-/-}$ and *Eif4ebp2*$^{-/-}$ mice were obtained as previously described [22, 24] and were both maintained on a C57BL/6J genetic background. Mice were housed under standard conditions (food/water available ad libitum, 22–25°C, 12 hour light:12 hour dark cycle [LD12:12]). *Eif4ebp2*$^{+/+}$ and *Eif4ebp2*$^{-/-}$ mice were obtained by breeding heterozygous mice. However, to speed up breeding throughput, *Eif4ebp1*$^{+/+}$ and *Eif4ebp1*$^{-/-}$ mice were bred separately. Nine *Eif4ebp1*$^{+/+}$ (26.5 ± 2.3 g, 69.1 ± 0.8 days) and 11 *Eif4ebp1*$^{-/-}$ (27.7 ± 2.1 g, 70.6 ± 3.7 days) nonlittermates were used for EEG/EMG recordings and gene expression measurements. Twelve *Eif4ebp2*$^{+/+}$ (29.0 ± 2.6 g, 77.4 ± 10.7 days) and 13 *Eif4ebp2*$^{-/-}$ (28.5 ± 3.3 g, 77.9 ± 11.4 days) littermates were used for EEG/EMG recordings and gene expression measurements. After electrode implantation surgery, recovery and adaptation to cabling (see below), the EEG and EMG were recorded continuously for 48 hours starting at light onset (Zeitgeber time 0 [ZT0]) comprising 24 hours of undisturbed conditions, a 6-hour SD starting at light onset (ZT0) and performed by gentle handling as described previously [25], and 18 hours following SD. Mice were then uncabled and half of the animals were submitted to a second SD from ZT0 to ZT6 one week later immediately followed by sacrifice and brain sampling together with the other half of animals that was sacrificed after undisturbed conditions. The prefrontal cortex of the left and right hemispheres was rapidly dissected and frozen on dry ice. Four *Eif4ebp2*$^{+/+}$ and four *Eif4ebp2*$^{-/-}$ not used for EEG/EMG recording were added for gene expression measurements. The protocol was performed in strict accordance with guidelines of the Canadian Council on Animal Care and approved by the Comité d'éthique de l'expérimentation animale of the Hôpital du Sacré-Coeur de Montréal (CIUSSS-NIM).

Electrode implantation surgery

EEG and EMG electrode implantation was performed as detailed previously [26–28]. Briefly, when mice reached 9–10 weeks, surgeries were performed under deep Ketamine/Xylazine anesthesia (120/10 mg/kg, i.p. injection) and followed by analgesia with Meloxicam (5 mg/kg, s.c. injection) and Bupivacaine (1.5 mg/kg, s.c. injection). Two gold-plated screws (diameter: 1.1 mm), screwed through the skull over the right cerebral hemisphere (anterior: 1.5 mm lateral to midline, 1.5 mm anterior to bregma; posterior: 1.5 mm lateral to midline, 1.0 mm anterior to lambda), served as EEG electrodes. An additional screw placed on the right hemisphere (2.6 mm lateral to midline, 0.7 mm posterior to bregma) served as a reference. Three anchors screws were implanted over the left hemisphere. Two gold wires were inserted between neck muscles to serve as EMG electrodes. The EEG and EMG electrodes were soldered to a connector and, together with the anchor screws, cemented to the skull. Four days after surgery, mice were connected to a swivel contact and animals were allowed a week of habituation to cabling conditions before recording.

EEG recording and analyses

The EEG and EMG signals were amplified (Lamont amplifier), sampled at 256 Hz and filtered using the commercial software Harmonie (Natus, Middleton, WI) as done previously [26–28]. Vigilance states (wakefulness, SWS, and PS) were visually assigned to 4-second epoch as described before [29]. Artifacts were simultaneously identified and subsequently excluded from spectral analysis. Vigilance state duration was averaged for the first 12 hours (light period, ZT0 to ZT12), the second 12 hours (dark period, ZT12 to ZT24), and per hour for baseline (i.e. the first 24 hours of recording under undisturbed conditions) and recovery (i.e. the second 24 hours of recording comprising the 6-hour SD and 18 hours of recovery). The mean duration of individual bouts of vigilance states was also computed for the 12-hour light and 12-hour dark periods during baseline. For the recovery day, the total duration of SWS during SD was calculated as well as the latency to the first 10 epochs (40 seconds) of SWS after the end of the 6-hour SD.

Spectral analysis was performed using fast Fourier transform to calculate the EEG power density between 0.5 and 50 Hz (0.25-Hz bins) on the bipolar EEG signal of artifact-free epochs for wakefulness, SWS and PS. Power spectra were computed for the full 24 hours of baseline and recovery and expressed as a percentage of the mean all-state EEG power of all frequencies during baseline for each mouse. To remove the large difference in amplitude between lower and higher frequencies for genotype comparison, spectral activity in each bin for each mouse was also normalized to the mean of wild-type mice. Normalized spectral activity was then averaged for six standard frequency bands for statistical comparisons (i.e. delta 1–4 Hz, theta 6–9 Hz, sigma 10–13 Hz, low beta 16–24 Hz, high beta 24–32 Hz, and gamma 32–50 Hz). Spectral activity was also separately computed for delta (1–4 Hz) and sigma (10–13 Hz) frequency bands during SWS and for the theta (6–9 Hz) band during wakefulness for time course analyses. To take into account the distribution of wakefulness and sleep, the spectral activity in these three bands was averaged per interval containing an equal number of epochs of a given state as performed previously [27, 30]. More precisely, SWS delta and sigma activity were computed for 12 equal intervals during the light period, 6 equal intervals during the dark periods, and 8 equal intervals during the 6-hour light period following SD. Wakefulness theta activity was average for 6 equal intervals during the light period, 12 equal intervals during the dark periods, 8 equal intervals during the 6-hour SD, and 3 equal intervals during the 6-hour light period following SD. The activity in the three frequency bands was expressed as a percentage of the mean of 24-hour baseline for each mouse.

Reverse transcription and qPCR

RNA extraction, reverse transcription, and qPCR were performed similar to described elsewhere [26, 27]. Briefly, RNA was extracted from one prefrontal cortex per mouse using the RNeasy Lipid Tissue Mini kit (Qiagen, Toronto, ON, Canada). The quality of RNA samples was assessed using agarose gel electrophoresis and the quantity with a NanoDrop 2000 spectrophotometer (Thermo Fisher Scientific, Waltham, MA). For reverse transcription, 250 ng of RNA was used with random hexamers and Superscript II reverse transcriptase (Invitrogen/Thermo Fisher Scientific, Burlington, ON, Canada) according to manufacturer's procedures. Gene expression was quantified for nine target genes (*Arc*, *Bdnf*, *Fos*, *Homer1a*, *Eif4ebp1*, *Eif4ebp2*, *Nrxn1*, *Nrxn2*, *Nrxn3*). *Arc*, *Bdnf*, *Fos*, and *Homer1a* have been selected because of their well-established increase under conditions of SD [9, 10, 13, 26, 27, 30], *Eif4ebp1* and *Eif4ebp2* expression has been measured to confirm the absence of transcript in KO mice and to assess the effect of SD on their gene expression, and *Nrxns* have been included to explore synaptic components relevant to sleep loss [8]. Each mouse complementary DNA (cDNA) was diluted and used in 10-µl reaction with Fast TaqMan Master Mix reagent (Applied Biosystems/Thermo Fisher Scientific) under standard cycling conditions: 50°C for 2 minutes followed by 40 cycles of 95°C for 1 second and 60°C for 20 seconds (ViiA7 real-time cycler, Life Technologies/Thermo Fisher Scientific). Primers were purchased from Invitrogen, Life Technologies or Operon (Huntsville, AL) and probes from Invitrogen or Operon. Taqman Gene Expression Assay numbers and sequences of designed oligos are listed in Table 1. The relative mRNA expression was calculated using the modified ΔΔCt method of Expression Suite v1.0.3 (Life Technologies), with the first Δ calculated using four endogenous control genes (i.e. *Actin*, TATA box binding protein [*Tbp*], Beta-glucuronidase [*GusB*], and Ribosomal protein S9 [*Rps9*]) and the second Δ using means of nonsleep-deprived wild-type mice.

Statistical analyses

Statistica 6.1 (StatSoft Inc./Tibco Software Inc., Palo Alto, CA) was used to perform statistical analyses and Prism 7 (GraphPad Software Inc., La Jolla, CA) to prepare figures. Vigilance state variables calculated for the 12-hour light and 12-hour dark periods, and vigilance state variables specific to SD were compared between genotypes for both *Eif4ebp1* and *Eif4ebp2* by Student's *t*-tests. Differences in vigilance state duration per hour, in normalized spectral activity per frequency bands and in time courses of delta, theta, and sigma frequency bands between genotypes were assessed using two-way repeated-measure analyses of variance (rANOVAs; with factors Genotype and Hour, Genotype and Frequency band, and Genotype and

Table 1. Sequence of primers and probes, and reference number of probe sets used for qPCR

		Life Technologies reference number or sequence 5′ to 3′	GenBank accession number
Actin	Fwd	CTAAGGCCAACCGTGAAAAGAT	NM_007393
	Rev	CACAGCCTGGATGGCTACGT	
	Probe	TTGAGACCTTCAACACCCCAGCCATG	
Arc		Mm00479619_g1	NM_018790.3
Bdnf		Mm04230607_s1	NM_007540.4
Eif4ebp1		Mm04207378_g1	NM_007918.3
Eif4ebp2		Mm00515675_m1	NM_010124.2
Fos		Mm00487425_m1	NM_010234.2
GusB	Fwd	ACGGGATTGTGGTCATCGA	NM_010368
	Rev	TGACTCGTTGCCAAAACTCTGA	
	Probe	AGTGTCCCGGTGTGGGCATTGTG	
Homer1a	Fwd	GCATTGCCATTTCCACATAGG	NM_011982
	Rev	ATGAACTTCCATATTTATCCACCTTACTT	
	Probe	ACACATTCAATTCAGCAATCATGA	
Nrxn1		Mm00660298_m1	NM_020252.3
Nrxn2		Mm01236851_m1	NM_001205234.1
Nrxn3		Mm04279482_m1	NM_001198587
Rps9	Fwd	GACCAGGAGCTAAAGTTGATTGGA	NM_029767
	Rev	TCTTGGCCAGGGTAAACTTGA	
	Probe	AAACCTCACGTTTGTTCCGGAGTCCATACT	
Tbp	Fwd	TTGACCTAAAGACCATTGCACTTC	NM_013684
	Rev	TTCTCATGATGACTGCAGCAAA	
	Probe	TGCAAGAAATGCTGAATATAATCCCAAGCG	

Interval, respectively). Significant effects were adjusted for repeated measures using the Huynh–Feldt correction. For time courses of EEG activity in frequency bands, rANOVAs were performed separately for the light and dark periods, given that two *Eif4ebp1*$^{+/+}$ mice and one *Eif4ebp2*$^{-/-}$ mouse presented an absence of SWS during the baseline dark period and one *Eif4ebp2*$^{+/+}$ mouse an absence of SWS during the recovery dark period. In addition, one *Eif4ebp2*$^{-/-}$ mouse was excluded from all recovery analyses because of continuous artifacts on the EEG. The effects of Genotype and SD on mRNA expression were evaluated by two-way factorial ANOVA (fANOVA). Significant interactions were decomposed using planned comparisons. The threshold for statistical significance was set to .05, and results are reported as mean ± SEM.

Results

More time spent in sleep in *Eif4ebp1*$^{-/-}$ mice

During baseline, *Eif4ebp1*$^{-/-}$ spent less time in wakefulness (~67 minutes less) and more time in SWS (~61 minutes more) than *Eif4ebp1*$^{+/+}$ only during the 12-hour dark period (Figure 1A). *Eif4ebp1*$^{-/-}$ mice were thus not significantly different from wild-type mice for wakefulness and SWS during the 12-hour light period and also expressed similar PS amount during the light and dark periods. In contrast, *Eif4ebp2*$^{-/-}$ mice were similar to *Eif4ebp2*$^{+/+}$ mice for all vigilance states during both the 12-hour light and dark periods. The 24-hour distribution of wakefulness, SWS, and PS was also analyzed to assess whether modifications in the time spent in wakefulness and SWS during the dark phase in *Eif4ebp1*$^{-/-}$ mice resulted from a global effect or from changes at specific hours (Figure 1B). More time was spent in SWS in *Eif4ebp1*$^{-/-}$ mice compared with wild-type mice mostly at the end of the dark period (ZT20 and ZT23; significant Genotype-by-Hour interaction). This was accompanied by less time spent in wakefulness at the same hours (significant interaction). Moreover, the analysis of the hourly distribution revealed more time spent in PS in *Eif4ebp1*$^{-/-}$ compared with *Eif4ebp1*$^{+/+}$ mice for several hours during the nychthemeron (i.e. ZT1, ZT2, ZT5, and ZT23; significant Genotype-by-Hour interaction; Figure 1B). The 24-hour distribution of wakefulness, SWS, and PS was similar between *Eif4ebp2*$^{-/-}$ and *Eif4ebp2*$^{+/+}$ mice.

The mean duration of individual bouts of the three vigilance states during baseline was calculated in *Eif4ebp1* and *Eif4ebp2* mice as an index of sleep consolidation/fragmentation. Longer and fewer bouts are usually a marker of consolidated wakefulness and sleep, whereas fragmented wake/sleep is reflected by more frequent and brief bouts. During the 12-hour dark period, *Eif4ebp1*$^{-/-}$ mice had longer PS bouts (~23 seconds longer) than wild-type mice (Figure 1C). This may have contributed to the increased time spent in PS observed for some hours during the dark phase (Figure 1B). No change was observed for the 12-hour light period. KO of *Eif4ebp2* did not modified the duration of individual bouts of vigilance states. Also, no change was observed for the number of bouts in any of the vigilance states (data not shown), supporting an overall preservation of the consolidation of wakefulness and sleep in the absence of 4E-BP1 or 4E-BP2. In summary, these results indicate that *Eif4ebp1*$^{-/-}$ mice have altered wakefulness and sleep amount, which is mostly due to changes occurring during the late active/dark period.

Altered EEG activity in *Eif4ebp1*$^{-/-}$ and *Eif4ebp2*$^{-/-}$ mice

Spectral analysis of the EEG was performed to verify whether *Eif4ebp1* and *Eif4ebp2* deletions affect the quality of wakefulness and sleep states (Figure 2). The deletion of *Eif4ebp1*

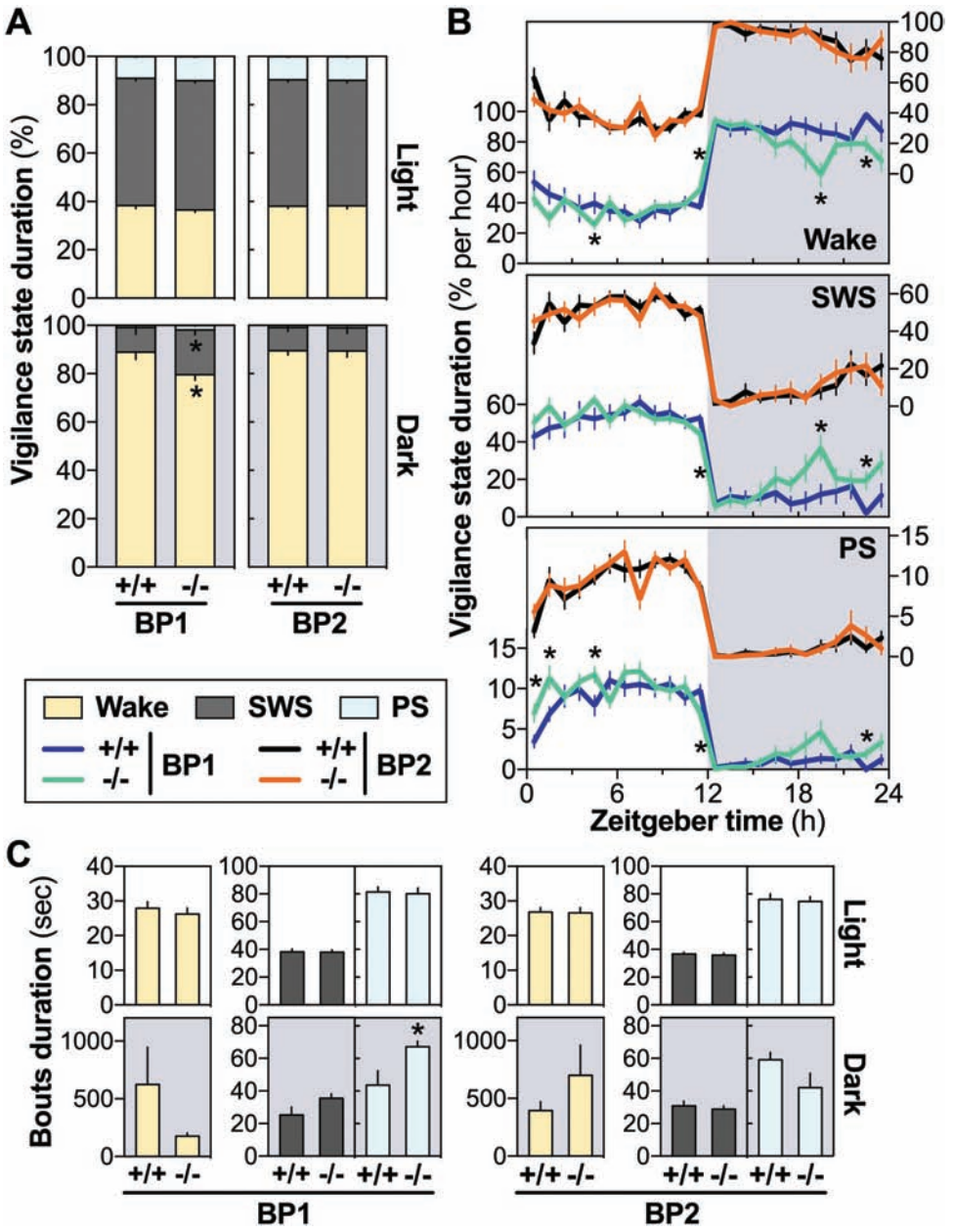

Figure 1. Baseline sleep architecture in *Eif4ebp1*$^{-/-}$ (BP1$^{-/-}$) and *Eif4ebp2*$^{-/-}$ (BP2$^{-/-}$) mice. (A) Proportion of time spent in wake, SWS, and PS for the 12-h light and 12-h dark periods. Wake and SWS percent were significantly different between BP1$^{+/+}$ and BP1$^{-/-}$ mice during the 12-h dark period ($t = \pm 2.5$, $^{*}p = .02$). No significant difference was found for the light period ($-0.7 < t < 1.2$, $p > .2$) or for PS ($-2.1 < t < -1.9$, $p > .05$) or for BP2 ($-0.5 < t < 0.3$, $p > .6$). Gray backgrounds indicate the 12-h dark period (also in B and C). (B) Time spent in wake, SWS, and PS computed per hour (left y-axes for BP1 and right y-axes for BP2). Genotype-by-Hour interactions were found for wake, SWS, and PS in the BP1 group (rANOVA: $F_{23,414} > 1.7$, $p \leq .02$; *t*-test: $^{*}p < .05$ between *bp1*$^{-/-}$ and *bp1*$^{+/+}$). No effect of Genotype (rANOVA: $F_{1,23} < 0.7$, $p > .4$) or interaction (rANOVA: $F_{23,529} < 1.0$, $p > .5$) was found for the BP2 group. (C) Mean duration of individual bouts of wake, SWS, and PS for the 12-h light and 12-h dark period. BP1$^{-/-}$ mice have longer PS bouts during the dark period ($t = -2.7$, $^{*}p = .02$). No significant difference was observed for BP1 during the light period for PS and for wake and SWS ($-2.0 < t < 2.0$, $p > .07$) and for all states in BP2 mice ($-1.1 < t < 1.7$, $p > .1$).

or *Eif4ebp2* engendered subtle effects on 24-hour EEG power spectra (Figure 2B). More precisely, during wakefulness, the absence of 4E-BP1 showed a tendency for lower spectral power than wild-type mice in all frequency bands (Genotype effect $p < .08$). During SWS, *Eif4ebp1*$^{-/-}$ mice did not significantly differ from wild-type mice in the power spectrum. During PS, a tendency for a Genotype-by-Frequency band interaction was found ($p = .08$ [$p < .04$ without Huynh–Feldt correction]). *Eif4ebp1*$^{-/-}$ mice appeared to have less spectral power in the delta frequency band (1–4 Hz) and more power in the theta band (6–9 Hz) in comparison to *Eif4ebp1*$^{+/+}$ mice. Conversely, *Eif4ebp2*$^{-/-}$ mice showed tendencies for more spectral power than wild-type littermates for all frequency bands during wakefulness and PS (Genotype effects $p = .09$ and $p = .06$, respectively), which seems particularly apparent for higher frequencies (low beta 16–24 Hz, high beta 24–32 Hz, and gamma 32–50 Hz) during wakefulness and delta and beta frequency bands during PS (Figure 2B). The *Eif4ebp2* deletion did not significantly change the power spectrum of SWS. In sum, the absence of 4E-BP1 tends to generally decrease synchronized

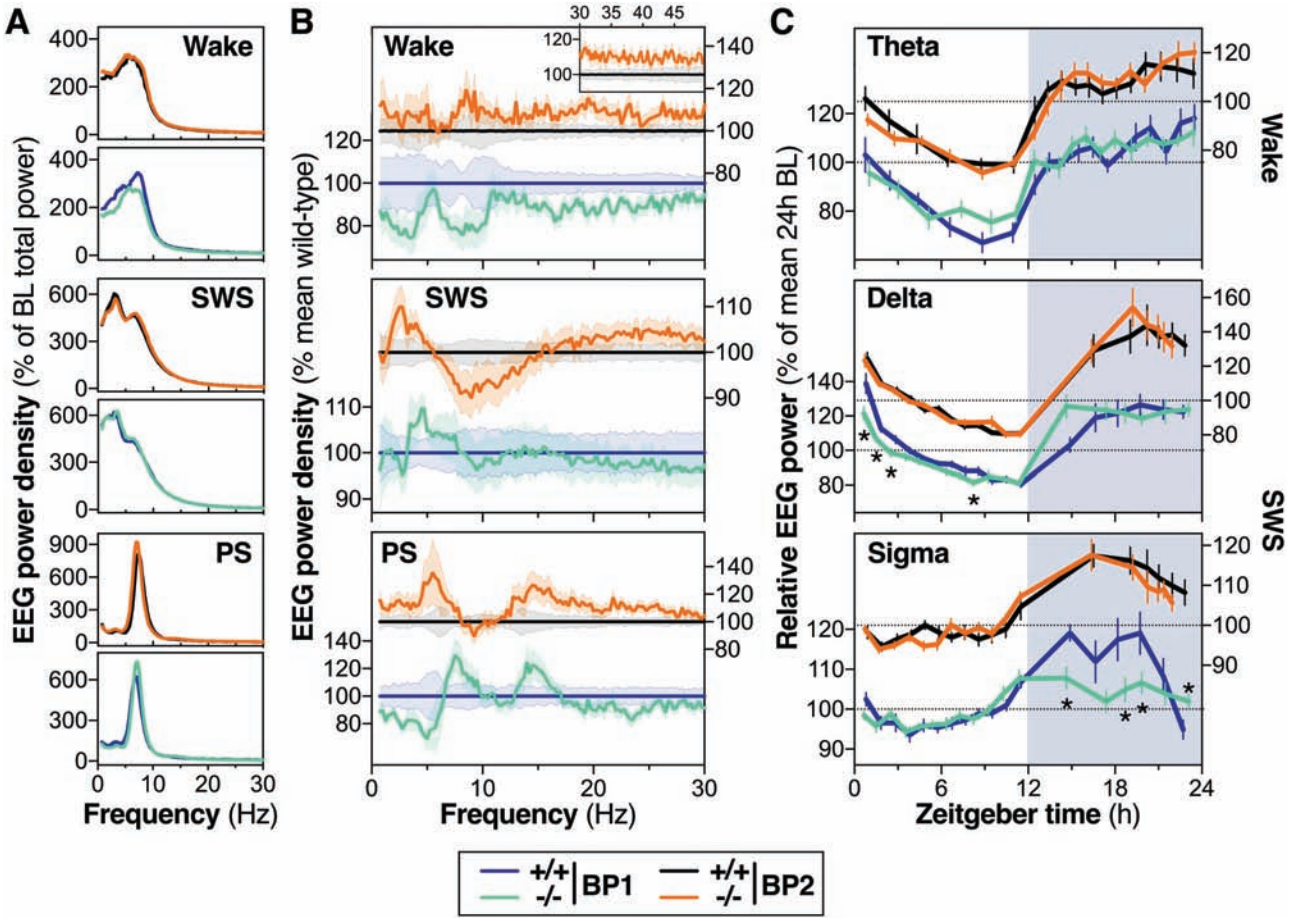

Figure 2. Baseline EEG activity in *Eif4ebp1*$^{-/-}$ (BP1$^{-/-}$) and *Eif4ebp2*$^{-/-}$ (BP2$^{-/-}$) mice. (A) Twenty-four-hour power spectra of wake, SWS, and PS in BP1$^{+/+}$, BP1$^{-/-}$, BP2$^{+/+}$, and BP2$^{-/-}$ mice. Errors bars have been omitted for clarity. (B) Spectral power represented for wake, SWS, and PS in percent mean BP1$^{+/+}$ or BP2$^{+/+}$ mice (left y-axes for BP1 and right y-axes for BP2; also in C). BP1$^{+/+}$ and BP1$^{-/-}$ did not significantly differ in spectral power during wakefulness (Genotype effect: $F_{1,18} = 3.5$, $p < .08$; Genotype-by-Frequency band interaction: $F_{5,90} = 1.4$, $p = .2$), SWS (Genotype effect: $F_{1,18} = 0.1$, $p = .8$; interaction: $F_{5,90} = 0.1$, $p = .9$), and PS (Genotype effect: $F_{1,18} = 0.3$, $p = .6$; interaction: $F_{5,90} = 2.5$, $p = .08$). Similarly, BP2$^{+/+}$ and BP2$^{-/-}$ did not significantly differ in spectral power during wakefulness (Genotype effect: $F_{1,23} = 3.1$, $p = .09$; interaction: $F_{5,115} = 0.04$, $p = .99$), SWS (Genotype effect: $F_{1,23} = 0.05$, $p = .8$; interaction: $F_{5,115} = 1.5$, $p = .2$), and PS (Genotype effect: $F_{1,23} = 3.9$, $p < .06$; interaction: $F_{5,115} = 0.9$, $p = .5$). Data for higher frequencies (30–50 Hz) are only represented for BP2 mice in wake because of no apparent difference for the other vigilance states and genotypes. (C) Twenty-four-hour time course of wake theta (6–9 Hz), SWS delta (1–4 Hz), and SWS sigma (10–13 Hz) activity in BP1$^{+/+}$, BP1$^{-/-}$, BP2$^{+/+}$, and BP2$^{-/-}$ mice. For theta, a Genotype-by-Interval interaction was found for *Eif4ebp1* mice during the 12-h light period (rANOVA: $F_{5,90} = 3.1$, $p = .02$), but not during the dark period (rANOVA: $F_{11,198} = 0.8$, $p = .6$). For BP1, Genotype-by-Interval interactions were also found for delta activity during the light period (rANOVA: $F_{11,187} = 3.4$, $p = .01$; *t*-tests: $^*p < .05$ between BP1$^{-/-}$ and BP1$^{+/+}$) and for sigma activity during the dark period (rANOVA: $F_{5,75} = 4.3$, $p = .002$; *t*-tests: $^*p < .05$ between BP1$^{-/-}$ and BP1$^{+/+}$), but not for delta during the dark and sigma during the light (rANOVA: $F_{5/11,80/198} < 1.2$, $p > .3$). No interaction reached statistical significance for BP2 mice (rANOVA: $F_{5/11,110/115/253} \leq 1.5$, $p \geq .1$). Gray backgrounds indicate the 12-h dark period.

cortical activity during wakefulness and PS during baseline, whereas the absence of 4E-BP2 tends to increase it for these two states.

Next, to better characterize markers of sleep regulatory processes, we examined the 24-hour time course of spectral activity in specific frequency bands. The time courses of wakefulness theta (6–9 Hz), SWS delta (1–4 Hz), and SWS sigma (10–13 Hz) activity were significantly different in *Eif4ebp1*$^{-/-}$ mice compared with *Eif4ebp1*$^{+/+}$ mice (Figure 2C). Indeed, a Genotype-by-Interval interaction revealed a modified time course of theta activity during the light period for wakefulness in *Eif4ebp1*$^{-/-}$ mice that likely results from alterations in relative changes between intervals because there was no specific interval for which genotypes significantly differ. Then, *Eif4ebp1*$^{-/-}$ mice expressed a decrease of delta activity for specific intervals during the light period, especially located at the beginning of the light period and thus potentially suggesting a lower level of homeostatic sleep pressure at the beginning of the rest period. Finally, a blunted light–dark rhythm of sigma activity appeared in *Eif4ebp1*$^{-/-}$ mice, mostly resulting from lower activity during some intervals of the dark period. In contrast, the baseline time courses of wakefulness theta, SWS delta, and SWS sigma activity were completely conserved in *Eif4ebp2*$^{-/-}$ mice in comparison to *Eif4ebp2*$^{+/+}$ mice (Figure 2C).

Altered EEG response to SD in *Eif4ebp2*$^{-/-}$ mice

To further explore the role of 4E-BP1 and 4E-BP2 in sleep homeostasis, we next measured the EEG response to SD in KO mice. During SD, *Eif4ebp1*$^{-/-}$ and *Eif4ebp2*$^{-/-}$ mice were deprived from the same amount of SWS (on average > 94%) in comparison to corresponding wild-type mice (Figure 3A, upper panel). The latency to SWS after SD was also similar between *Eif4ebp1*$^{-/-}$ and *Eif4ebp2*$^{-/-}$ mice and wild-type mice (Figure 3A, bottom panel). Similar to

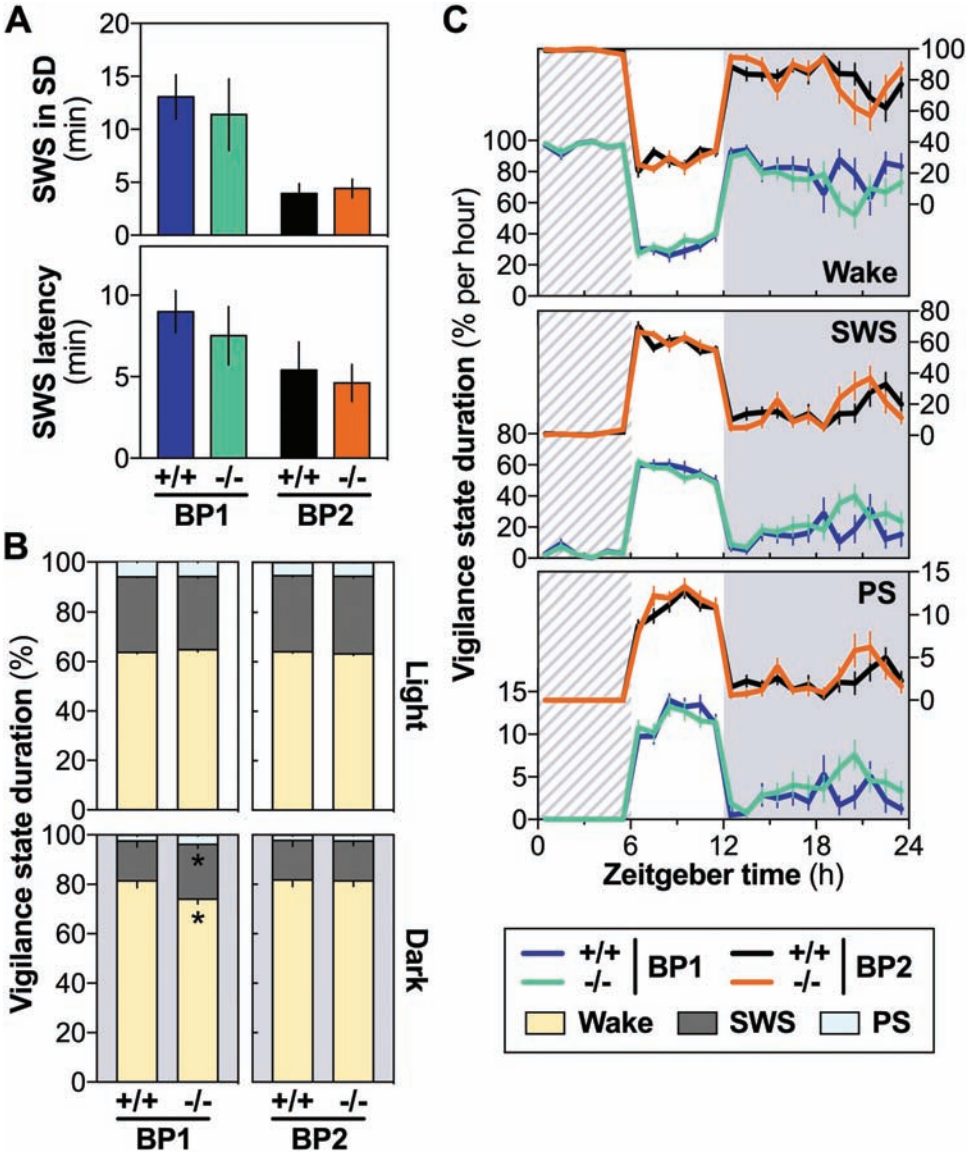

Figure 3. Sleep architecture parameters during and after SD in *Eif4ebp1*$^{-/-}$ (BP1$^{-/-}$) and *Eif4ebp2*$^{-/-}$ (BP2$^{-/-}$) mice. (A) SWS during SD and latency to SWS after SD did not significantly differ between genotypes in both BP1 and BP2 groups (SWS during SD: $t \leq 0.6$, $p \geq .5$; SWS latency: $t \leq 0.5$, $p \geq .6$). (B) Proportion of time spent in wake, SWS, and PS for the 12-h light and 12-h dark periods. Wake and SWS percent were significantly different between BP1$^{+/+}$ and BP1$^{-/-}$ mice during the 12-h dark period ($t = \pm 2.2$, $^{*}p = .04$). No difference was found for the light period ($t = \pm 1.1$, $p = .3$) or for PS ($-2.1 < t < 0.5$, $p > .06$) or for BP2 ($-1.4 < t < 1.2$, $p > .19$). Gray backgrounds indicate the 12-h dark period (also in C). (C) Time spent in wake, SWS, and PS computed per hour (left y-axes for BP1 and right y-axes for BP2). No genotype effect or Genotype-by-Hour interaction was found for wake, SWS, and PS in the BP1 group (Genotype: $F_{1,18} < 4.1$, $p > .05$; interaction: $F_{17/23,306/414} < 1.6$, $p > .08$) or in the BP2 group (Genotype: $F_{1,22} < 1.1$, $p > .3$; interaction: $F_{23/17,506/374} < 1.4$, $p > .1$). Hatched areas represent the 6-h SD.

observations made for baseline, *Eif4ebp1*$^{-/-}$ mice spent less time in wakefulness (~54 minutes) and more time in SWS (~43 minutes) than *Eif4ebp1*$^{+/+}$ mice during the 12-hour dark period following SD (Figure 3B). However, the time courses of the three vigilance states were no longer significantly different between *Eif4ebp1*$^{-/-}$ and *Eif4ebp1*$^{+/+}$ mice for the 24-hour recovery (Figure 3C), which indicates a global effect of the mutation. Also similar to baseline observations, *Eif4ebp2*$^{-/-}$ mice did not significantly differ from *Eif4ebp2*$^{+/+}$ mice in time spent in vigilance states and in 24-hour distribution of vigilance states (Figure 3, B and C).

Next, EEG power spectra and time courses of activity in frequency bands during and after SD revealed fewer genotype differences in comparison with baseline data for *Eif4ebp1*$^{-/-}$ mice but more differences in comparison to baseline for *Eif4ebp2*$^{-/-}$ mice (Figure 4, A and B). First, similar to baseline, *Eif4ebp1*$^{-/-}$ mice showed a tendency for lower power in all frequency bands during wakefulness in comparison to *Eif4ebp1*$^{+/+}$ mice (Genotype effect $p = .1$), similar SWS power and a tendency for lower delta power and higher theta power during PS (interaction $p < .1$; Figure 4B). Also similar to baseline, *Eif4ebp2*$^{-/-}$ mice presented more spectral power than wild-type littermates for all frequency bands during both wakefulness and PS (Figure 4B). However, these *Eif4ebp2* genotype differences reached statistical significance during recovery, which was not the case during baseline.

During recovery, the time courses of wake theta activity, of SWS delta activity, and of SWS sigma activity did not differ between

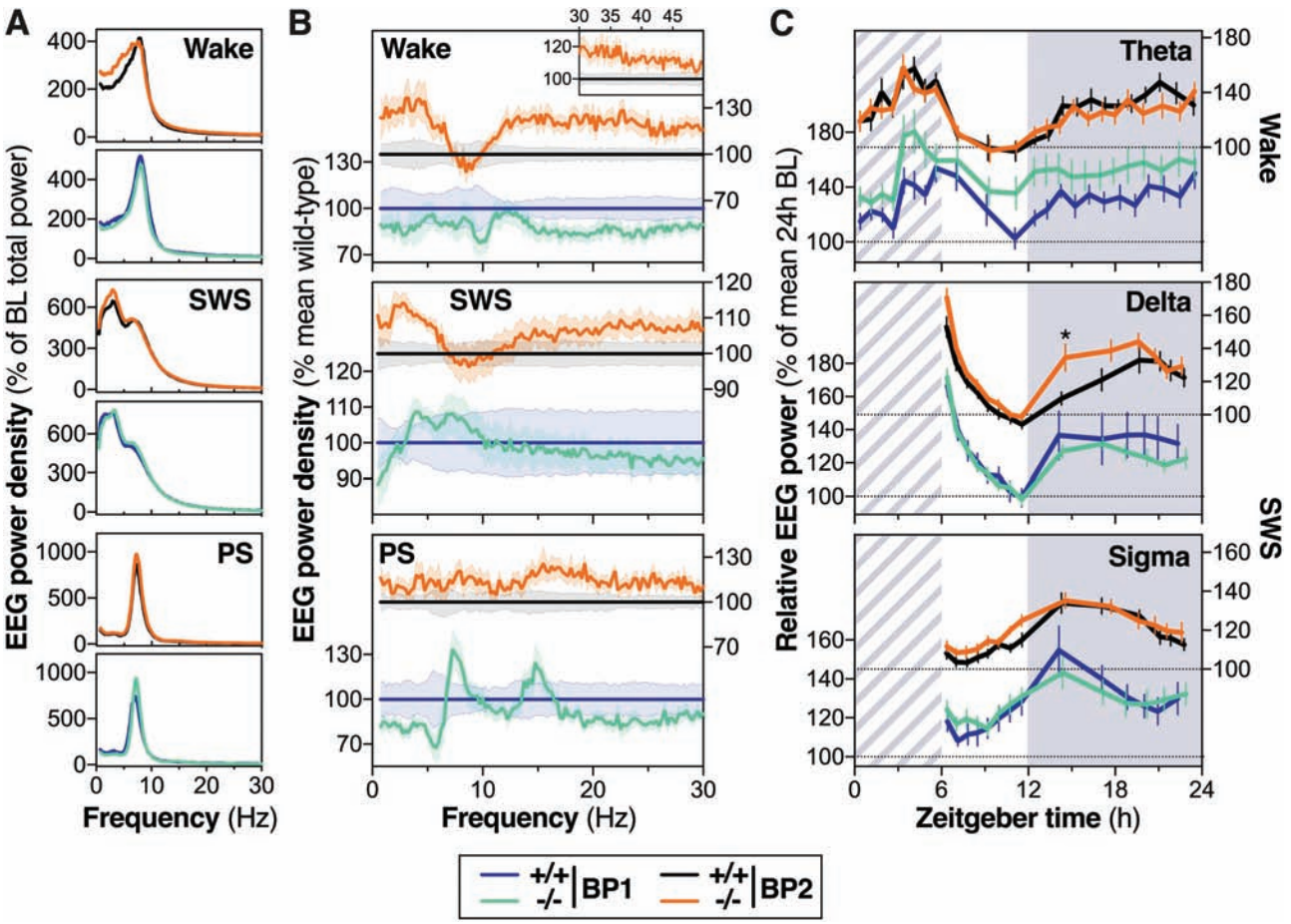

Figure 4. EEG activity during and after SD in *Eif4ebp1*$^{-/-}$ (BP1$^{-/-}$) and *Eif4ebp2*$^{-/-}$ (BP2$^{-/-}$) mice. (A) Twenty-four-hour power spectra of wake, SWS, and PS in BP1$^{+/+}$, BP1$^{-/-}$, BP2$^{+/+}$, and BP2$^{-/-}$ mice. Errors bars have been omitted for clarity. (B) Spectral power represented for wake, SWS, and PS in percent mean BP1$^{+/+}$ or BP2$^{+/+}$ mice (left y-axes for BP1 and right y-axes for BP2; also in C). BP1$^{+/+}$ and BP1$^{-/-}$ did not significantly differ in spectral power during wakefulness (Genotype effect: $F_{1,18} = 2.4$, $p = .1$; Genotype-by-Frequency band interaction: $F_{5,90} = 0.3$, $p = .9$), SWS (Genotype effect: $F_{1,18} = 0.01$, $p = .9$; interaction: $F_{5,90} = 0.6$, $p = .7$), and PS (Genotype effect: $F_{1,18} = 0.7$, $p = .4$; interaction: $F_{5,90} = 2.0$, $p = .09$). BP2$^{+/+}$ and BP2$^{-/-}$ significantly differed in spectral power during wakefulness (Genotype effect: $F_{1,22} = 7.6$, $p = .01$; interaction: $F_{5,110} = 2.5$, $p = .06$) and PS (Genotype effect: $F_{1,22} = 6.5$, $p = .02$; interaction: $F_{5,110} = 0.4$, $p = .8$), but not during SWS (Genotype effect: $F_{1,22} = 1.5$, $p = .2$; interaction: $F_{5,110} = 1.7$, $p = .15$). Data for higher frequencies (30–50 Hz) are only represented for BP2 mice in wake because of no apparent difference for the other vigilance states and BP1 genotypes. (C) Twenty-four-hour time course of wake theta (6–9 Hz), SWS delta (1–4 Hz), and SWS sigma (10–13 Hz) activity in BP1$^{+/+}$, BP1$^{-/-}$, BP2$^{+/+}$, and BP2$^{-/-}$ mice. For theta activity, no Genotype effect (rANOVA: $F_{1,18} \leq 2.7$, $p \geq .1$) or Genotype-by-Interval interaction (rANOVA: $F_{10/11,180/198} \leq 1.5$, $p \geq .1$) was found for BP1 mice, but a Genotype-by-Interval interaction was found for the dark phase in BP2 mice (rANOVA: $F_{11,242} = 1.9$, $p = .04$). For delta activity, no Genotype effect ($F_{1,18} \leq 0.7$, $p \geq .4$) or Genotype-by-Interval interaction ($F_{5/7,90/126} \leq 1.1$, $p \geq .4$) was found for BP1, but a significant Genotype-by-Interval interaction was found for the dark phase in BP2 ($F_{5,105} = 3.8$, $p = .005$; *t*-test: $^*p = .02$). For sigma activity, no Genotype effect (BP1: $F_{1,18} \leq 0.4$, $p \geq .5$; BP2: $F_{1,21/22} \leq 3.1$, $p \geq .09$) or Genotype-by-Interval interaction (BP1: $F_{5/7,90/126} \leq 0.8$, $p \geq .08$; BP2: $F_{5/7,105/154} \leq 1.2$, $p \geq .3$) was found. Gray backgrounds indicate the 12-h dark period.

Eif4ebp1$^{-/-}$ and *Eif4ebp1*$^{+/+}$ mice (Figure 4C). The time course of wake theta was different between *Eif4ebp2*$^{-/-}$ and *Eif4ebp2*$^{+/+}$ mice for the dark phase during recovery, but this was not associated with significant genotype differences at precise intervals. The analysis of the SWS delta activity time course in response to SD revealed an altered time course in *Eif4ebp2*$^{-/-}$ mice compared with *Eif4ebp2*$^{+/+}$ mice (Figure 4C). More precisely, *Eif4ebp2*$^{-/-}$ mice expressed an increased relative delta activity at the beginning of the recovery dark period. This result could be due to the observation that these mice had more wakefulness in the first 2 hours of the dark period following SD than *Eif4ebp2*$^{+/+}$ mice (from ZT12 to ZT14; $t = 2.3$, $p = .03$; see Figure 3C), which should result in an increased homeostatic sleep pressure. Similar to *Eif4ebp1*, the SWS sigma activity time course during recovery was not significantly modified by the *Eif4ebp2* deletion. Globally, the EEG activity response to SD is mostly unaffected by the *Eif4ebp1* deletion, whereas it appears to be amplified by the *Eif4ebp2* deletion.

Altered gene expression response to SD in *Eif4ebp1*$^{-/-}$ mice

We investigated the effects of the absence of 4E-BP1 or 4E-BP2 on the expression of selected genes following SD to assess their potential contribution to the molecular response to SD. To do so, we measured mRNA steady-state levels at ZT6 of nine genes in the prefrontal cortex of mice immediately following SD and of mice left undisturbed (controls). Consistent with previous literature [9, 10, 13, 26, 27, 30], the expression of the immediate early (plasticity-related) genes *Arc*, *Fos*, and *Homer1a* was increased by SD in comparison to undisturbed conditions (Figure 5). The KO of *Eif4ebp1* or of *Eif4ebp2* did not affect this increase. The previously reported SD-induced increase in *Bdnf* gene expression [9, 26, 27, 31] was also observed in *Eif4ebp2*$^{-/-}$ and *Eif4ebp2*$^{+/+}$ mice but did not reach statistical significance in *Eif4ebp1*$^{-/-}$ and *Eif4ebp1*$^{+/+}$ mice. This last observation may be due the apparent complete lack of SD-induced increase in *Eif4ebp1*$^{-/-}$ mice.

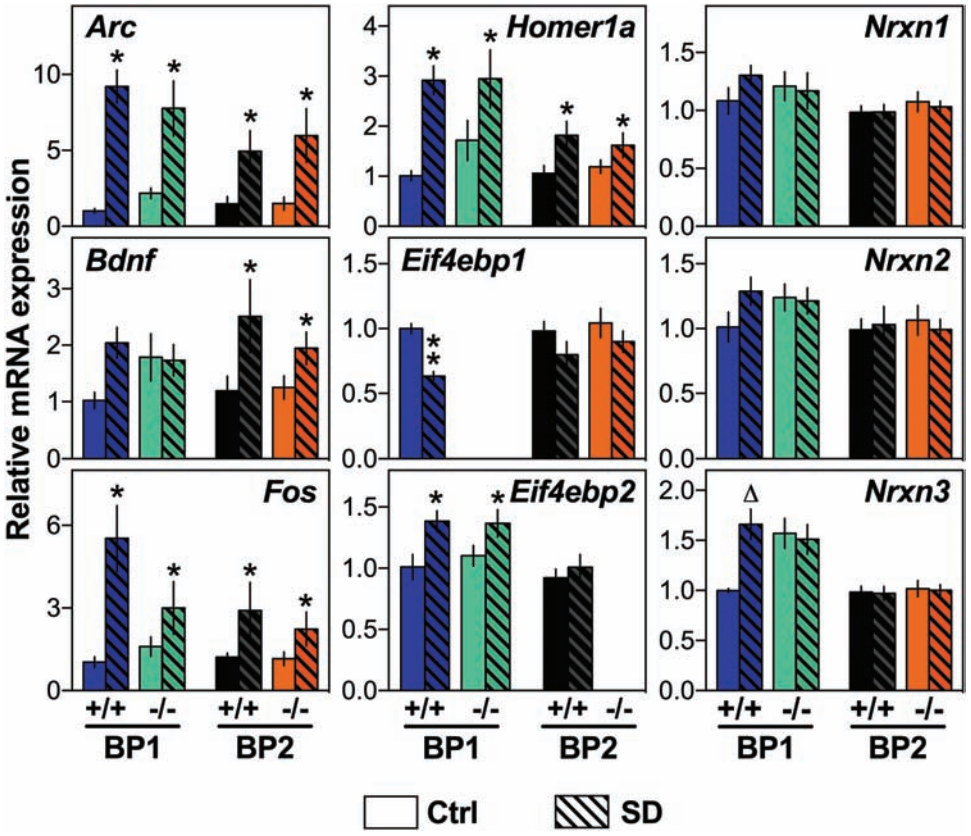

Figure 5. Expression of target genes after SD in the prefrontal cortex of *Eif4ebp1*$^{-/-}$ (BP1$^{-/-}$) and *Eif4ebp2*$^{-/-}$ (BP2$^{-/-}$) mice. Relative levels of steady-state mRNA were measured by qPCR under undisturbed conditions (Ctrl: BP1$^{-/-}$ $n = 6$, BP1$^{+/+}$ $n = 3$, BP2$^{-/-}$ $n = 9$, BP2$^{+/+}$ $n = 8$) or after a 6-h sleep deprivation (SD: BP1$^{-/-}$ $n = 5$, BP1$^{+/+}$ $n = 5$, BP2$^{-/-}$ $n = 8$, BP2$^{+/+}$ $n = 8$). In BP1 mice, a significant SD effect was found for *Arc*, *Fos*, *Homer1a*, and *Eif4ebp2* (fANOVA: $F_{1,15} \geq 9.95$, $^{*}p < .007$) as well as for *Eif4ebp1* (*t*-test: $t = 6.1$, $^{**}p = .0009$), but not for *Bdnf* (fANOVA: $F_{1,15} = 2.3$, $p = .15$). Also, a significant Genotype-by-SD interaction was found for *Nrxn3* (fANOVA: $F_{1,15} = 5.5$, $p = .03$; $^{\Delta}p = .01$ compared with Ctrl). In BP2 mice, only significant SD effects were found for *Arc*, *Bdnf*, *Fos*, and *Homer1a* (fANOVA: $F_{1,28/30} \geq 4.9$, $^{*}p \leq .04$).

The expression of *Eife4bp1* mRNA was not detectable in *Eif4ebp1*$^{-/-}$ mice, as the expression of *Eif4ebp2* mRNA in *Eif4ebp2*$^{-/-}$ mice, confirming the absence of the transcripts (Figure 5). SD decreased the mRNA level of *Eife4bp1* in *Eif4ebp1*$^{+/+}$ mice and increased the expression of *Eif4ebp2* in *Eif4ebp1*$^{-/-}$ and *Eif4ebp1*$^{+/+}$ mice. The expression of *Nrxn3*, which encodes a synaptic adhesion protein located at the presynapse, was significantly increased by SD in *Eif4ebp1*$^{+/+}$ mice, but not in *Eif4ebp1*$^{-/-}$ mice, likely resulting from a high mRNA level under baseline conditions in *Eif4ebp1*$^{-/-}$ mice (Figure 5). The expression of genes coding for the related presynaptic proteins *Nrxn1* and *Nrxn2* was not significantly changed by SD or by the *Eif4ebp1* and *Eif4ebp2* deletions. Overall, SD-induced changes in prefrontal gene expression are slightly attenuated in the absence of 4E-BP1 but preserved in the absence of 4E-BP2.

Discussion

In the present study, we used electrophysiology and molecular biology to investigate the effects of the absence of either 4E-BP1 or 4E-BP2 on wakefulness and sleep quantity and quality as well as on well-characterized homeostatic responses to sleep loss. We report multiple modifications in wakefulness and sleep quantity and quality in *Eif4ebp1*$^{-/-}$ mice comprising more time spent in SWS during the active period and modified time course of spectral activity in various frequency bands during wakefulness and SWS under undisturbed conditions. This was associated with a modest attenuation of the gene expression response to SD. On the other hand, *Eif4ebp2*$^{-/-}$ mice showed alterations in wakefulness and sleep phenotypes restricted to spectral activity during wakefulness and sleep mainly revealed under high sleep pressure conditions. Together, these results highlight the implication of specific translational control effectors in sleep regulation and suggest different roles for 4E-BP1 and 4E-BP2 in the regulation of wakefulness and sleep.

As indicated in the introduction, there are three 4E-BPs (1, 2, and 3), and it is not feasible to study various deletions and their combinations in a single study. Given that 4E-BP1 and 4E-BP2 are more important in the brain, we selectively studied them independently to compare their roles in sleep regulation. Contrary to our expectations vis-a-vis the association between 4E-BP2 and autistic-like behaviors [23], the absence of 4E-BP2 did not engender a sleep phenotype similar to patients with autism (e.g. less time spent in SWS, decreased sleep consolidation) [1, 2]. Indeed, the sleep architecture was strikingly similar in *Eif4ebp2*$^{+/+}$ and *Eif4ebp2*$^{-/-}$ mice, both under baseline and sleep-deprived conditions. This could be explained by a marginal role of 4E-BP2 in brainstem and hypothalamic areas controlling wakefulness and sleep duration and alternation, such as the parabrachial nucleus and hypothalamic preoptic areas [32]. However, although 4E-BP1 is much less abundant in the brain than 4E-BP2 [20, 22], its absence had greater impact on wakefulness and sleep duration.

More precisely, the absence of 4E-BP1 was detrimental to wakefulness and resulted in increased sleep states, which was particularly manifested in the active/dark period. As indicated in the introduction, 4E-BP1 is expressed in the SCN and plays a role in the functioning of the circadian timing system [21]. The SCN was shown to have outputs directed to brainstem areas of the ascending arousal system, such as the locus coeruleus [33]. It is thus possible that altered circadian function in *Eif4ebp1*$^{-/-}$ mice [21] is accompanied by impaired circadian outputs to the arousal system resulting in decreased wakefulness. Our observation that the decrease in time spent in wakefulness is mainly observed during a specific time window within the 24-hour day (i.e. the second half of the active period) also supports the implication of the circadian timing system in mediating the effect of 4E-BP1 absence on wake/sleep architecture.

Along the same line, a strong circadian regulation of the activation of hypothalamic orexin cells was reported in mice [34] and the SCN has been shown to regulate the 24-hour rhythm in orexin level in the rat cerebrospinal fluid [35]. More precisely, the peak of orexin expression occurring during the late active/dark period was abolished by a lesion to the SCN [35]. Orexin neurons favor the transition to wakefulness [36]. Accordingly, an altered SCN function in *Eif4ebp1*$^{-/-}$ mice could change orexin transmission during the active/dark period and lead to less time spent in wakefulness at this "circadian" time. Nevertheless, *Eif4ebp1*$^{-/-}$ mice have higher level of vasoactive intestinal peptide (VIP) in the SCN [21], which could result in less sleep during the active/dark period given that *Vip* KO mice display more sleep specifically during this period [37]. It is noteworthy that, on the contrary, application of VIP to other brain regions was shown to enhance sleep [38, 39]. Targeted studies are required to differentiate the SCN-dependent and -independent roles of 4E-BP1 in the regulation of wakefulness and sleep.

Our results indicate that the quality of vigilance states assessed using spectral analysis of the EEG was modified by the absence of 4E-BP1 or of 4E-BP2. Concerning wakefulness specifically, their absence appeared to have opposite effects on spectral power. This is surprising given the similar role of these two translation repressors in cap-dependent translation [16] and in the neuronal organization of the cerebral cortex [40]. Moreover, the absences of 4E-BP1 and 4E-BP2 were both shown to increase the expression of the synaptic adhesion molecule Neuroligin-1 in the spinal cord and hippocampus, respectively [23, 41]. An increase in Neuroligin-1 level in the central nervous system would be expected to increase EEG spectral power in the theta/alpha range during wakefulness because we have shown that *Neuroligin-1* KO mice have lower power in these frequencies [26]. The tendency for *Eif4ebp1*$^{-/-}$ mice to have a reduced power in theta frequencies may thus suggest a mechanism independent of Neuroligin-1, which would also be supported by observations in vigilance states other than wakefulness. Findings in *Eif4ebp1*$^{-/-}$ mice should nevertheless be interpreted with caution given that nonlittermates were studied. In *Eif4ebp2*$^{-/-}$ mice, the tendency for increased spectral power in all frequency bands during wake could be linked to the reported synaptic alterations in these mice. Indeed, *Eif4ebp2*$^{-/-}$ mice have a facilitated hippocampal long term potentiation and present an increased ratio of synaptic excitation to inhibition [22, 23], which could both contribute to enhanced cortical synchronization captured in faster frequencies at the level of the wakefulness (and PS) EEG. Besides, cell type-specific roles of 4E-BP1 and 4E-BP2, as reported for immune cells [42], are likely contributing to their differential effects on the wakefulness and sleep EEG.

In parallel, modifications in outputs of the SCN to orexin neurons could also contribute to changes in EEG activity during wakefulness and sleep in *Eif4ebp1*$^{-/-}$ mice because *orexin* KO mice were shown to express multiple alterations in the spectral composition of the wakefulness and SWS EEG [43]. It is also interesting to note that mTOR seems part of an intracellular signaling pathway mediating orexin neurotransmission [44]. This could support, as also raised above, a role for 4E-BPs in modulating EEG activity via the orexin system independent of the circadian timing system. Nonetheless, alteration in the amplitude of the 24-hour time course of SWS sigma activity in *Eif4ebp1*$^{-/-}$ mice could also be linked to a circadian dysfunction because the daily dynamics of SWS sigma activity has been associated with the circadian regulation of sleep [5, 6, 45]. Given that SWS sigma activity is indicative of sleep spindles [5, 45], our specific observation of decreased sigma during the baseline dark period in *Eif4ebp1*$^{-/-}$ mice may point to a decreased circadian drive for spindles at this time of the day.

The time course of SWS delta activity, a marker of sleep homeostasis [5, 45], was also modified in *Eif4ebp1*$^{-/-}$ mice in comparison to *Eif4ebp1*$^{+/+}$ mice. In particular, *Eif4ebp1*$^{-/-}$ mice showed lower delta activity at the beginning of the rest/light period, which could indicate lower homeostatic sleep pressure to start their resting phase. This lower pressure could easily be explained by the enhanced time spent in SWS at the end of the active/dark period in these mutant animals. In fact, when KO mice were deprived from the same amount of sleep as wild-type mice (i.e. using SD), a preserved homeostatic response to SD was observed in the absence of 4E-BP1. This is reminiscent of alterations in the baseline dynamics of SWS delta activity together with an intact SWS delta activity rebound after SD in *orexin* KO mice [43]. Unlike *Eif4ebp1*$^{-/-}$ mice, the absence of 4E-BP2 resulted in more modifications of EEG activity during wakefulness and sleep under homeostatically challenged/sleep-deprived conditions in comparison to wild-type mice. In particular, *Eif4ebp2*$^{-/-}$ mice showed significantly more activity during both wakefulness and sleep, which was not present during baseline and, concerning SWS delta activity in particular, seemed to predominate 6 hours after the end of SD. These contrasting effects of SD in the absence of 4E-BP1 or 4E-BP2 further support roles of the two repressors in different sleep regulatory circuits and/or cell types. In parallel, different subcellular localization of these translational repressors may differently shape neuronal excitability in the neocortex and consequently EEG activity under increased homeostatic sleep pressure. 4E-BP2 indeed appears to be enriched at postsynaptic sites and lower in dendritic shafts in comparison to 4E-BP1 in hippocampal neurons in culture [46].

Similar to our observation of contrasting EEG responses to SD in *Eif4ebp1*$^{-/-}$ versus *Eif4ebp2*$^{-/-}$ mice, their gene expression was differently changed by SD. SD was previously shown to decrease the level of phosphorylated 4E-BP2 in the hippocampus but to leave total 4E-BP2 level intact [14]. Similarly, SD was shown to decrease the level of phosphorylated 4E-BP1 in the visual cortex following monocular deprivation in comparison to sleep [15]. These two studies highlighted roles for 4E-BPs in sleep-dependent plasticity in two different brain areas. However, in the present study, the mRNA expression of *Eif4ebp1* and *Eif4ebp2* in the prefrontal cortex is changing in opposite directions with SD, with *Eif4ebp1* being decreased and *Eif4ebp2* increased. In line with overall trends in power spectra modifications in *Eif4ebp1*$^{-/-}$ and *Eif4ebp2*$^{-/-}$ mice, this observation supports different roles of these two translation repressors in sleep regulation (or similar

roles in different cell types). Of interest is also that the gene expression response to SD appears to be altered by the absence of 4E-BP1 specifically. In fact, the increased expression of precise genes related to synaptic function and plasticity was no longer observed in *Eif4ebp1*$^{-/-}$ mice, which appears to result from elevated expression under baseline conditions. This finding supports the previously proposed role for 4E-BP1 in wake/sleep-related modifications of neuronal plasticity [15].

Several observations support the conclusion that protein synthesis/regulation is affected by wakefulness and sleep history [47, 48]. This is illustrating the role of the sleep/wake cycle in the regulation of required cellular mechanisms such as translation and represents an explanation for the deleterious effects of sleep loss on functions depending on protein synthesis (e.g. memory consolidation, some forms of neuronal plasticity) [14, 15, 47]. Our current findings are supporting a bidirectional relationship between wakefulness/sleep and the translation machinery by highlighting that the absence of translational repressors affects wakefulness and sleep quality as quantified using EEG spectral analysis. Assessing the role of mTOR itself in the regulation of the wakefulness and sleep EEG, for instance by recording the EEG of viable mTOR heterozygous mice, will help to understand the more global role of the protein synthesis machinery in wakefulness and sleep regulation as well as the pathophysiology of sleep disturbances in brain diseases involving mTORopathy [49, 50]. Our study warrants future research to evaluate the contribution of the role of the mTOR pathway in nervous system development [19] in the sleep phenotype of *Eif4ebp1*$^{-/-}$ and *Eif4ebp2*$^{-/-}$ mice by, for instance, studying genetic inactivation or overexpression of translational repressors performed at different developmental ages. Importantly, such strategy will also allow investigating brain region- and cell type-specific roles of 4E-BPs to better understand the specific roles of 4E-BP1 and 4E-BP2 in the regulation of wakefulness and sleep.

Acknowledgments

The authors are thankful to A. Sylvestre, E. Bélanger-Nelson, C. Provost, C. Bouchard, D. Petit, and G. Poirier for technical help and to colleagues who have provided help with SD (J. Dufort-Gervais, L. Hannou, B. S. Seok, E. K. O'Callaghan, and N. Lemmetti).

Funding

The research has been supported by M.Sc. fellowships of the Department of Neuroscience and of the Faculty of Medicine of the Université de Montréal to C.C.A., salary awards from the Canadian Institutes of Health Research (CIHR) and the Fonds de Recherche du Québec-Santé to V.M., the Canada Research Chair in Sleep Molecular Physiology (V.M.), and a CIHR grant to N.S.

Conflict of interest statement. None declared.

References

1. Limoges E, *et al*. Atypical sleep architecture and the autism phenotype. *Brain*. 2005;**128**(Pt 5):1049–1061.
2. Ballester P, *et al*. Sleep problems in adults with autism spectrum disorder and intellectual disability. *Autism Res*. 2019;**12**(1):66–79.
3. Daan S, *et al*. Timing of human sleep: recovery process gated by a circadian pacemaker. *Am J Physiol*. 1984;**246**(2 Pt 2):R161–R183.
4. Borbély AA, *et al*. The two-process model of sleep regulation: a reappraisal. *J Sleep Res*. 2016;**25**(2):131–143. doi:10.1111/jsr.12371
5. Dijk DJ, *et al*. Contribution of the circadian pacemaker and the sleep homeostat to sleep propensity, sleep structure, electroencephalographic slow waves, and sleep spindle activity in humans. *J Neurosci*. 1995;**15**(5 Pt 1):3526–3538.
6. Yasenkov R, *et al*. Interrelations and circadian changes of electroencephalogram frequencies under baseline conditions and constant sleep pressure in the rat. *Neuroscience*. 2011;**180**:212–221.
7. Rachalski A, *et al*. Contribution of transcriptional and translational mechanisms to the recovery aspect of sleep regulation. *Ann Med*. 2014;**46**(2):62–72.
8. Areal CC, *et al*. Sleep loss and structural plasticity. *Curr Opin Neurobiol*. 2017;**44**:1–7.
9. Cirelli C, *et al*. Extensive and divergent effects of sleep and wakefulness on brain gene expression. *Neuron*. 2004;**41**(1):35–43.
10. Mackiewicz M, *et al*. Macromolecule biosynthesis: a key function of sleep. *Physiol Genomics*. 2007;**31**(3):441–457.
11. Ramm P, *et al*. Rates of cerebral protein synthesis are linked to slow wave sleep in the rat. *Physiol Behav*. 1990;**48**(5):749–753.
12. Nakanishi H, *et al*. Positive correlations between cerebral protein synthesis rates and deep sleep in *Macaca mulatta*. *Eur J Neurosci*. 1997;**9**(2):271–279.
13. Vecsey CG, *et al*. Genomic analysis of sleep deprivation reveals translational regulation in the hippocampus. *Physiol Genomics*. 2012;**44**(20):981–991.
14. Tudor JC, *et al*. Sleep deprivation impairs memory by attenuating mTORC1-dependent protein synthesis. *Sci Signal*. 2016;**9**(425):ra41.
15. Seibt J, *et al*. Protein synthesis during sleep consolidates cortical plasticity in vivo. *Curr Biol*. 2012;**22**(8):676–682.
16. Sonenberg N, *et al*. Regulation of translation initiation in eukaryotes: mechanisms and biological targets. *Cell*. 2009;**136**(4):731–745.
17. Burnett PE, *et al*. RAFT1 phosphorylation of the translational regulators p70 S6 kinase and 4E-BP1. *Proc Natl Acad Sci USA*. 1998;**95**(4):1432–1437.
18. Gingras AC, *et al*. eIF4 initiation factors: effectors of mRNA recruitment to ribosomes and regulators of translation. *Annu Rev Biochem*. 1999;**68**:913–963.
19. Swiech L, *et al*. Role of mTOR in physiology and pathology of the nervous system. *Biochim Biophys Acta*. 2008;**1784**(1):116–132.
20. Tsukiyama-Kohara K, *et al*. Tissue distribution, genomic structure, and chromosome mapping of mouse and human eukaryotic initiation factor 4E-binding proteins 1 and 2. *Genomics*. 1996;**38**(3):353–363.
21. Cao R, *et al*. Translational control of entrainment and synchrony of the suprachiasmatic circadian clock by mTOR/4E-BP1 signaling. *Neuron*. 2013;**79**(4):712–724.
22. Banko JL, *et al*. The translation repressor 4E-BP2 is critical for eIF4F complex formation, synaptic plasticity, and memory in the hippocampus. *J Neurosci*. 2005;**25**(42):9581–9590.
23. Gkogkas CG, *et al*. Autism-related deficits via dysregulated eIF4E-dependent translational control. *Nature*. 2013;**493**(7432):371–377.
24. Tsukiyama-Kohara K, *et al*. Adipose tissue reduction in mice lacking the translational inhibitor 4E-BP1. *Nat Med*. 2001;**7**(10):1128–1132.

25. Franken P, *et al*. Sleep deprivation in rats: effects on EEG power spectra, vigilance states, and cortical temperature. *Am J Physiol*. 1991;**261**(1 Pt 2):R198–R208.
26. El Helou J, *et al*. Neuroligin-1 links neuronal activity to sleep-wake regulation. *Proc Natl Acad Sci USA*. 2013;**110**(24):9974–9979.
27. Freyburger M, *et al*. EphA4 is involved in sleep regulation but not in the electrophysiological response to sleep deprivation. *Sleep*. 2016;**39**(3):613–624.
28. Seok BS, *et al*. The effect of neuroligin-2 absence on sleep architecture and electroencephalographic activity in mice. *Mol Brain*. 2018;**11**(1):52.
29. Franken P, *et al*. Genetic determinants of sleep regulation in inbred mice. *Sleep*. 1999;**22**(2):155–169.
30. Curie T, *et al*. Homeostatic and circadian contribution to EEG and molecular state variables of sleep regulation. *Sleep*. 2013;**36**(3):311–323.
31. Mongrain V, *et al*. Separating the contribution of glucocorticoids and wakefulness to the molecular and electrophysiological correlates of sleep homeostasis. *Sleep*. 2010;**33**(9):1147–1157.
32. Saper CB, *et al*. Wake-sleep circuitry: an overview. *Curr Opin Neurobiol*. 2017;**44**:186–192.
33. Aston-Jones G, *et al*. A neural circuit for circadian regulation of arousal. *Nat Neurosci*. 2001;**4**(7):732–738.
34. Marston OJ, *et al*. Circadian and dark-pulse activation of orexin/hypocretin neurons. *Mol Brain*. 2008;**1**:19.
35. Zhang S, *et al*. Lesions of the suprachiasmatic nucleus eliminate the daily rhythm of hypocretin-1 release. *Sleep*. 2004;**27**(4):619–627.
36. Adamantidis AR, *et al*. Neural substrates of awakening probed with optogenetic control of hypocretin neurons. *Nature*. 2007;**450**(7168):420–424.
37. Bedont JL, *et al*. An LHX1-regulated transcriptional network controls sleep/wake coupling and thermal resistance of the central circadian clockworks. *Curr Biol*. 2017;**27**(1):128–136.
38. Bourgin P, *et al*. Rapid eye movement sleep induction by vasoactive intestinal peptide infused into the oral pontine tegmentum of the rat may involve muscarinic receptors. *Neuroscience*. 1999;**89**(1):291–302.
39. Simón-Arceo K, *et al*. Long-lasting enhancement of rapid eye movement sleep and pontogeniculooccipital waves by vasoactive intestinal peptide microinjection into the amygdala temporal lobe. *Sleep*. 2003;**26**(3):259–264.
40. Lin TV, *et al*. Normalizing translation through 4E-BP prevents mTOR-driven cortical mislamination and ameliorates aberrant neuron integration. *Proc Natl Acad Sci USA*. 2016;**113**(40):11330–11335.
41. Khoutorsky A, *et al*. Translational control of nociception via 4E-binding protein 1. *Elife*. 2015;**4**:e12002. doi:10.7554/eLife.12002
42. So L, *et al*. The 4E-BP-eIF4E axis promotes rapamycin-sensitive growth and proliferation in lymphocytes. *Sci Signal*. 2016;**9**(430):ra57.
43. Vassalli A, *et al*. Hypocretin (orexin) is critical in sustaining theta/gamma-rich waking behaviors that drive sleep need. *Proc Natl Acad Sci USA*. 2017;**114**(27):E5464–E5473.
44. Wang Z, *et al*. Orexin/hypocretin activates mTOR complex 1 (mTORC1) via an Erk/Akt-independent and calcium-stimulated lysosome v-ATPase pathway. *J Biol Chem*. 2014;**289**(46):31950–31959.
45. Dijk DJ, *et al*. Variation of electroencephalographic activity during non-rapid eye movement and rapid eye movement sleep with phase of circadian melatonin rhythm in humans. *J Physiol*. 1997;**505** (Pt 3):851–858.
46. Tang SJ, *et al*. A rapamycin-sensitive signaling pathway contributes to long-term synaptic plasticity in the hippocampus. *Proc Natl Acad Sci USA*. 2002;**99**(1):467–472.
47. Seibt J, *et al*. Translation regulation in sleep: making experience last. *Commun Integr Biol*. 2012;**5**(5):491–495.
48. Diering GH, *et al*. Homer1a drives homeostatic scaling-down of excitatory synapses during sleep. *Science*. 2017;**355**(6324):511–515.
49. Bruni O, *et al*. Sleep disorders in tuberous sclerosis: a polysomnographic study. *Brain Dev*. 1995;**17**(1):52–56.
50. van Eeghen AM, *et al*. Characterizing sleep disorders of adults with tuberous sclerosis complex: a questionnaire-based study and review. *Epilepsy Behav*. 2011;**20**(1):68–74.